Structural Characterization of Porous and Granular Materials

R. Hihinashvili* (Imperial College London) & R. Blumenfeld (Imperial College London/University of Cambridge)

SUMMARY

The morphological details of permeable porous materials impact significantly their macro-scale properties and in particular transport properties (e.g. permeability). A programme to derive macroscopic behaviour and responses from pore-scale information is a holy grail in the field. We report here progress on, and tests of, a recently proposed such a programme.

The main steps of the programme are as follows. The solid phase of a porous material is first skeletonised into a framework of nodes and edges. Then the local structure is quantified by means of structure tensors, which describe the shape of novel volume elements called quadrons. Next, the local tensor description is used in an entropy-based statistical formalism to compute macroscopic structural characteristics as expectation values over a certain partition function. From the structural characteristics, physical properties can be evaluated. The 'thickened' structure is taken account of with an additional partition function, giving more accurate evaluation of structural and physical properties.

Here we present tests for the initial stages of the programme. The tests are carried out on numerically generated two-dimensional granular aggregates. Specifically, we describe results on the statistics of the quadrons and the structural tensors.

Introduction

Many industrial processes and applications rely on the performance of porous media ranging from porous rocks in oil recovery schemes (Dullien 1992) to porous electrodes in fuel cell technology (Brandon and Brett 2006). The physical properties of porous media, and specifically their transport properties, e.g. permeability and conductivity, depend heavily on their pore-scale structure. To understand and predict the behaviour of porous media, one must first quauntify the disordered microstructure usefully. This should then be used in a systematic method to infer macro-scale properties of porous media given their pore-scale structure.

Such a method has been proposed recently in two and three dimensions (Frenkel et al. 2008 and 2009), based on an entropic formalism to describe the statistics of the pore-scale structure (Blumenfeld and Edwards 2003 and 2006).

In this paper we first review the general method briefly and in particular the quantification of the structure. We then report results of the application of this method to describe the structural properties of model two-dimensional (2D) porous media.

Methodology

Quantification of the microstructure

Given a three-dimensional (3D) porous material, its *solid phase* is first skeletonized reducing it to a framework of nodes, connected by edges (e.g. the structure in Fig. 1). This framework is then transformed into a network of connected polyhedra, called the *contact network*. This is accomplished by joining the midpoints of the edges between nodes (see example in Fig. 2); the midpoints are the polyhedra vertices.

In this framework, the voids are represented by polyhedra (cells), whose surfaces are made of triangles and skew polygons. The triangles are the facets of the node polyhedra surrounding the void, and the skew polygons that they enclose are the (skeletal) throats to neighbouring voids.

The method is based on tessellating the volume of the medium by volume elements called *quadrons* (Blumenfeld and Edwards 2003 and 2006). We sketch the construction of one such element in Fig. 3. In 2D all quadrons are quadrilateral and in 3D octahedra. [1] The shape of a quadron is defined by a tensor, constructed of three vectors.

The three vectors relate a node, an adjacent cell and an adjacent throat (Fig. 3 (a)). One of these vectors corresponds to the edge of the node polyhedron. Its direction is such that if viewed from within the node polyhedron, it rotates clockwise arround the triangular facet. We denote it by $\mathbf{r}^{cvp}$ since it resides on cell c, the polyhedron of node v and the polygonal throat p. A second vector, $\boldsymbol{\xi}^{cvp}$, joins the centroid of a facet of the node polyhedron with the centroid of an adjacent polygonal throat (the centroid of a polygon/polyhedron is defined as the arithmetic mean of its vertices). A third vector, $\mathbf{R}^{cv}$, joins the centroid of the node polyhedron with the centroid of an adjacent cell (this vector is indexed uniquely by c and v). In terms of this vectors, the quadron shape tensor is defined as:

$$C^{cvp} = (\boldsymbol{\xi}^{cvp} \times \mathbf{r}^{cvp}) \otimes \mathbf{R}^{cv} \tag{1}$$

where $\times$ and $\otimes$ denote cross and outer products, respectively.

The structural features of a quadron are encoded by this tensor. For example, the volume of an octahedron is given by the trace of the corresponding tensor: $V^{cvp} = \frac{1}{6}|\text{Tr}\{C^{cvp}\}|$. The quadrons cover the volume perfectly, i.e. without overlaps or gaps.

---

[1] Except when the number of vertices around a polyhedron is smaller than 4.
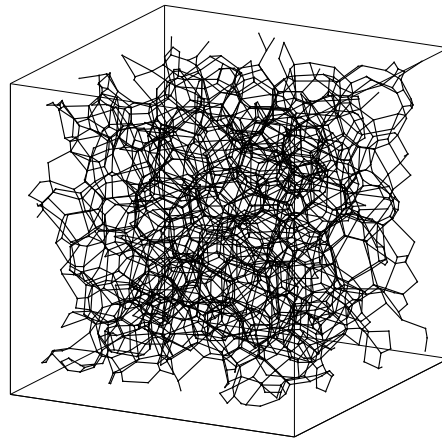
Figure 1: A numerically generated foam structure, represented as a framework of nodes connected by edges (Plateau borders). In foam structures, four edges meet at each node.
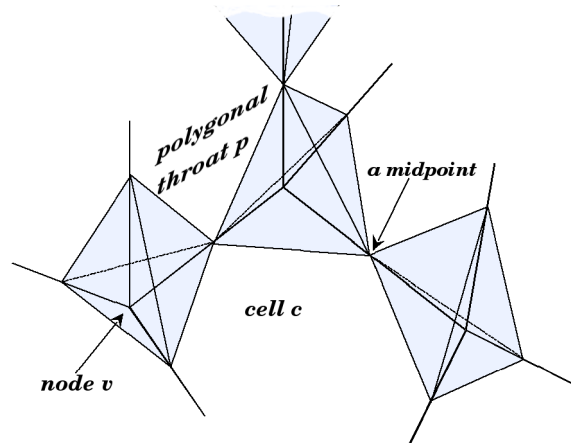
Figure 2: To construct the node polyhedra in a network structure, join the midpoints of edges between nodes around each node. In this picture, four edges meet at each node, therefore, the polyhedra that form are tetrahedra. The voids are represented by polyhedra (cells), whose surfaces are made of the facets (all are triangles by construction) of the node polyhedra surrounding the void, and the skew polygons that they enclose. The skew polygons are the (skeletal) throats to neighbouring voids.
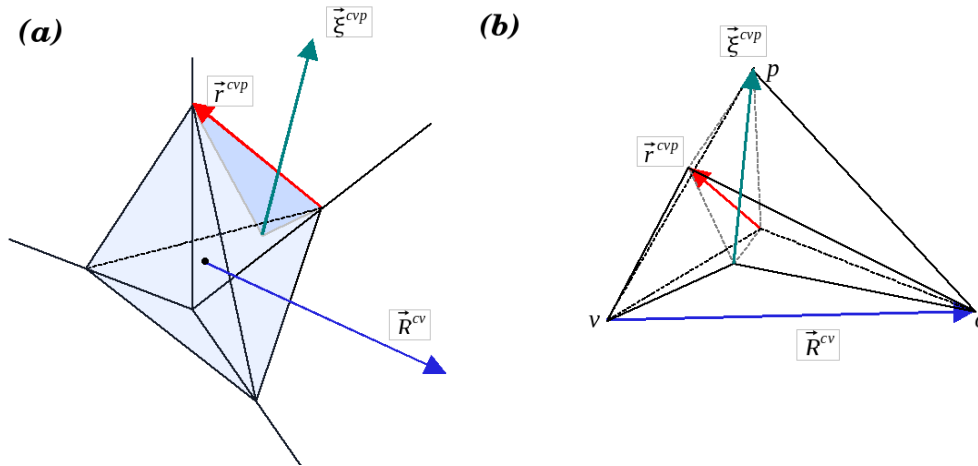
Figure 3: (a) Let us focus on one node and its vicinity. For instance, we consider the leftmost tetrahedron of Fig. 2. Three vectors are defined: a vector denoted by $\mathbf{r}^{cvp}$ joins two midpoints around the node (it is an edge of the tetrahedron); a vector denoted by $\boldsymbol{\xi}^{cvp}$ joins the centroid of a triangular facet of the tetrahedron with the centroid of an adjacent polygonal throat (the centroid of a polygon/polyhedron is the arithmetic mean of its vertices); and a vector denoted by $\mathbf{R}^{cv}$ joins the centroid of the node tetrahedron with the centroid of an adjacent cell. (b) The vectors $\mathbf{r}^{cvp}$ and $\boldsymbol{\xi}^{cvp}$ form a dihedral quadrilateral (a quadrilateral composed of two triangles that are not on the same plane). Join the four corners of this quadrilateral with the centroid of the node polyhedron (the 'tail' of $\mathbf{R}^{cv}$) and with the centroid of the cell (the head of $\mathbf{R}^{cv}$) to form two pyramids that share a base. The two pyramids form together a non-convex octahedron; this is a 3D quadron.

In two dimensions, the geometrical construction is conceptually the same, but clearly simpler. It involves only two vectors (see Fig. 4 (a)). The contact network comprises polygons circulating nodes. The polygon edges, denoted by $\mathbf{r}^{cv}$, join midpoints around nodes. They are also the edges of polygons around voids (cells). Extending a vector $\mathbf{R}^{cv}$ from the centroid of a node polygon to the centroid of an adjacent cell, we obtain another set of vectors. The pair of vectors $\mathbf{r}^{cv}$ and $\mathbf{R}^{cv}$ are the diagonals of a quadrilateral quadron; its shape tensor is defined as

$$C^{cv} = (\hat{\varepsilon}\mathbf{r}^{cv}) \otimes \mathbf{R}^{cv} \tag{2}$$

where $\hat{\varepsilon} = \left(\begin{smallmatrix} 0 & 1 \\ -1 & 0 \end{smallmatrix}\right)$. Similarly to 3D, C^{cv} quantifies the structure of a quadron, and in particular its area is: $V^{cv} = \frac{1}{2}|\text{Tr}\{C^{cv}\}|$. The anti-symmetric part of C^{cv} gives a measure of the deviation of the quadrilateral from a perfect rhombus (Ball and Blumenfeld 2002).

The geometric construction described above is also applicable to systems of granular aggregates (Fig. 4 (b)), where grains are identified with nodes and the inter-granular contacts with midpoints. In both cases, we construct a contact network and the quadron description follows. This makes it a unified description of both types of media.

This mathematical description of the structure benefits from several advantages. Firstly, it assigns numbers to every point in space. Secondly, it captures the connectivities of the solid phase and the pore space. Thirdly, The tensorial description captures local descriptors of the structure that are of interest, e.g. the throats and the surface area. Fourthly, all the quadrons are the same polytope – quadrilaterals in 2D and octahedra in 3D. This makes possible an unambiguous mathematical quantification, in contrast to Voronoi-based tessellation methods, commonly used to describe granular aggregates.

An application of this description is the following. Considering the cells that form around the voids and the polygonal throats that interconnect them, one can use the cell volumes and the throat areas as an input into a pore-scale network model (a spheres and 'tubes' model where the spheres represent pores and the tubes represent throats). Fig. 5 of (Frenkel et al. 2009) illustrates this application.
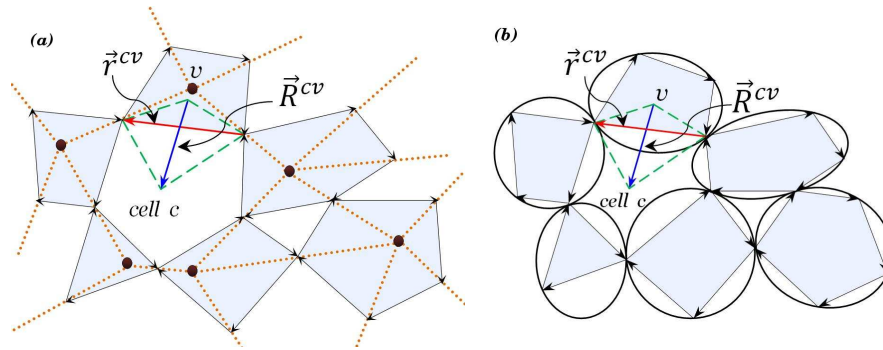
Figure 4: This figure illustrates (in 2D) how the same quantification applies both to (a) a framework of nodes connected by edges (exaggerated dots and dotted lines) and (b) a granular aggregate. The midpoints between nodes, or the inter-granular contact points, are joined by vectors $\mathbf{r}^{cv}$ to form polygons around nodes/grains. In this figure, both media are transformed into the same *contact network* – a network of connected polygons (colour filled). The quadrons are defined based on the contact network. The vectors $\mathbf{r}^{cv}$ also form polygons around the voids (*cells*). Extend a vector $\mathbf{R}^{cv}$ from the centroid of a node/grain polygon to the centroid of an adjacent cell. The vector $\mathbf{R}^{cv}$ and the vector $\mathbf{r}^{cv}$ that it crosses are the diagonals of a quadrilateral quadron (dashed line). A quadron is indexed by cv, namely, it belongs to node/grain v and cell c.

Furthermore, it is possible to analyse the statistics of the throat areas and cell volumes and use these to construct statistically equivalent such networks. The statistical method which allows us to calculate means is briefly reviewed in the following.

Upscaling from the pore scale

Since the quadrons tessellate the space, the sum of their volumes is the total volume of the system. A key observation is that they give the volume in terms of local variables (i.e. the vectors $\mathbf{r}^{cvp}$, $\boldsymbol{\xi}^{cvp}$ and $\mathbf{R}^{cv}$). This allows to use an entropy-based statistical formalism, initially proposed for granular aggregates (Edwards and Oakeshott 1989) and later extended to general network structures (Blumenfeld and Edwards 2006).

The entropic formalism makes it possible to evaluate structural properties on a scale larger than the pore-scale by calculating expectation values over a certain partition function. This formalism is analogous to statistical mechanics of thermodynamic systems. It is based on the assumption that all possible pore-scale configurations (microstates) are available. While in conventional thermodynamics a microstate is weighed by its energy, here it is weighed by its volume, provided by a volume function. Thus the quadrons are the 'quasi-particles' to use the language of statistical mechanics.

Using this formalism, we can calculate expectation values of any relevant structural property. For example, the expected distribution of the throat areas can be calculated to infer local permeabilities, or the distribution of surface areas, for inferring local heat conductivities. The entropic formalism makes it possible to go beyond the skeletal structure and take into account more realistic geometries of the solid phase. This is done by incorporating an additional statistical ensemble that describes the size and shape of grains that are overlaid on the node polyhedra. The same applies in the calculation of the throat areas or thickness of edges. Adding the geometric features leads for example to reduced throats (see Fig. 5).

Preliminary results

Two-dimensional granular aggregates

To illustrate the use of the method, examine it and develop it further, we apply it to numerically generated structures. For clarity, we choose to investigate first two-dimensional systems, which will provide insight
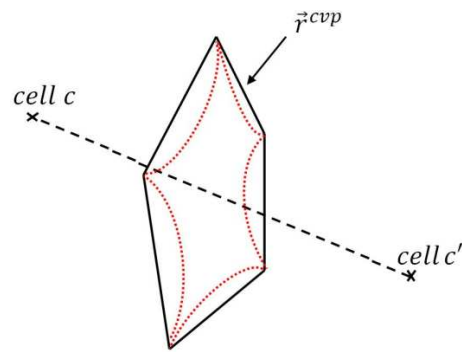
Figure 5: A sketch showing a polygonal throat (solid line) and a realistic throat (dashed line). In this example, the node polyhedra are overlaid with spherical grains. The area of the polygonal throat is obtained from the $\mathbf{r}^{cvp}$ vectors that form it. The realistic throat area is obtained from the vectors $\mathbf{r}^{cvp}$ and the radii of the spherical grains.
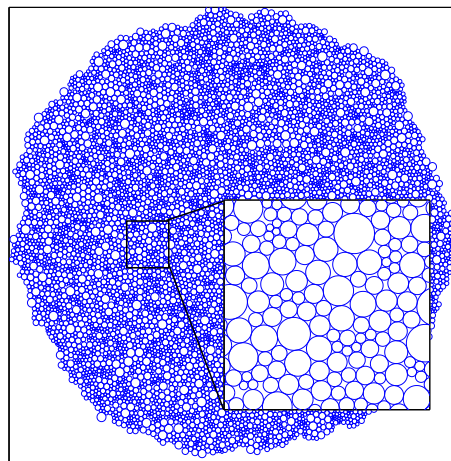

Figure 6: The model structure: a 2D dense granular aggregate with a size distribution as indicated by the probability density functions (PDF) in Fig. 8. In this figure, the aggregate comprises 10000, but the statistics presented are for aggregates that contain 500000 grains.

into the analysis in general, both in 2D and 3D.

For porous media made of particles, the construction described above requires data about individual grains and voids. Specifically, it requires knowledge of the inter-granular contacts and which grains surround each void. The granular aggregates were generated sequentially, with one grain added at a time. The construction is purely geometrical and does not involve simulation of physical processes (e.g. collisional or friction forces). The grains are discs, whose sizes are distributed according to a limit distribution (see below). With this algorithm, aggregates that comprise 500000 grains have been generated in few seconds.

Our aim was to study extreme cases – dense and sparse aggregates – and later compare with morphologies of intermediate densities. To make the aggregates as dense as possible, we maximised during the generation process the number of voids surrounded by exactly three grains (an example for such an aggregate with 10000 grains is shown in Fig. 6). Although our algorithm attempts to generate only such voids, this is not possible topologically for disc size distributions of finite support, and cells surrounded by more than 3 grains must form.
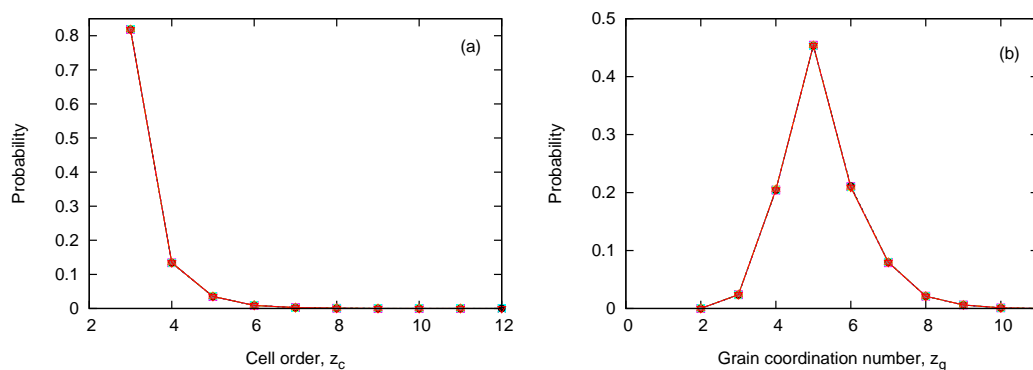
Figure 7: The (a) cell order (the number of grains around a void) and (b) the grain coordination number (the number of contacts of a grain) superposed PDF's of ten dense aggregates comprising 500000 grains each.
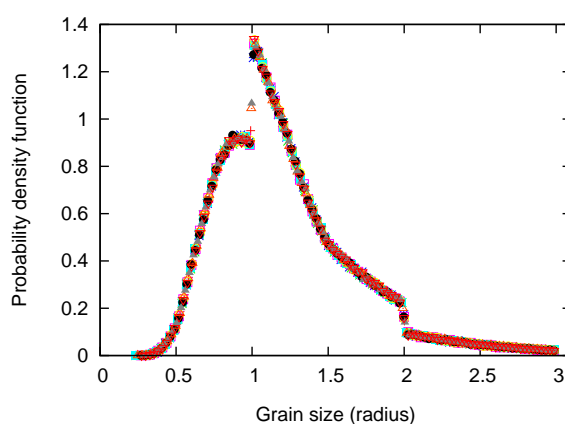
Figure 8: The grain size (radius) superposed PDF's of ten dense aggregates comprising 500000 grains each (same aggregates as in Fig. 7).

Fig. 7 shows the superposed probability density functions (PDF) of the number of discs around cells (cell order), from ten aggregates of 500000 grains each. Notice that over 80% of the cells are surrounded by three grains (cell order $z_c = 3$). The porosity of these packs is low indeed – 12.5%.

At the beginning of the construction, disc radii are chosen randomly from the interval $[R_{min}, R_{max}] = [1.0, 2.0]$. However, our algorithm allows self-consistent broadening of the distribution until it reaches the limiting form shown in Fig. 8. This form is robust, as evident by the superposition of the PDF's taken from ten aggregates.

We have quantified the microstructure of these systems in terms of quadrons and their shape tensors, and derived the distributions of the vectors $\mathbf{r}^{cv}$ and $\mathbf{R}^{cv}$ that define the quadrons. Fig. 9 (a) shows the quadron volume PDF's obtained for ten dense aggregates (the volumes are normalised by the mean grain area), and Fig. 9 (b) shows the PDF's of the angle α^{cv} between $\mathbf{r}^{cv}$ and $\mathbf{R}^{cv}$. The distribution of $sin(\alpha^{cv})$ (not shown here) peaks sharply at 1.0, meaning that these angles are distributed narrowly around $\pi/2$; the cosine PDF's show that the spread of angles around $\pi/2$ is fairly symmetric. PDF's of the magnitude of the $\mathbf{r}^{cv}$ vectors, normalized by the mean disc radius, are given in Fig. 9 (c).

Discussion

The results presented here are preliminary and aim only to illustrate the application of the structural characterisation method to a family of test structures. Specifically, we have analysed the statistics that
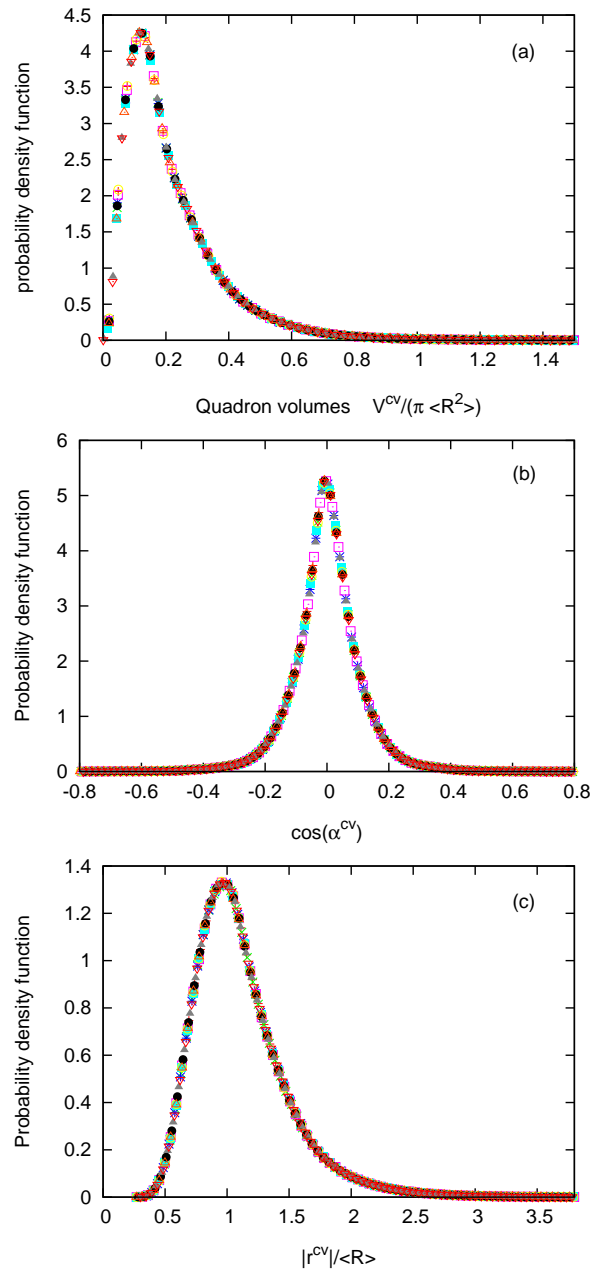
Figure 9: The (a) quadron volume, (b) the cosine of the angle α^{cv} between $\mathbf{r}^{cv}$ and $\mathbf{R}^{cv}$ and (c) the magnitude of $\mathbf{r}^{cv}$ superposed PDF's of ten dense aggregates comprising 500000 grains each (same aggregates as in Fig. 7). The quadron volumes are normalized by the mean grain area $\pi\langle R^2 \rangle$, and $|\mathbf{r}^{cv}|$ are normalized by the mean grain radius $\langle R \rangle$.

relate directly to the quantification of the microstructure by means of quadrons and their shape tensors.

Note that, at the level of the framework, there is a duality between the grain/node polygons and the cell polygons. One can regard the former as enclosing the latter and vice versa. Thus every such structure can represent, in principle, two different physical systems where the voids and solid phases interchange. Moreover, there is a relation between the mean cell order, $\bar{z}_c$, and the mean number of contacts per grain, $\bar{z}_g$: $\bar{z}_c = \frac{2\bar{z}_g}{\bar{z}_g - 2}$. In our aggregates, $\bar{z}_c \cong 3.245$ and $\bar{z}_g \cong 5.21$.

The inverse relation between $\bar{z}_c$ and $\bar{z}_g$ means that the denser the original pack the less dense the dual one. It follows that the structures that we have analysed of our dense disc aggregates correspond to very sparse dual granular systems, albeit of a different distribution of grain shapes and sizes. The same observation applies to 3D systems by interchanging the cell and node/grain polyhedra – an issue we have started to look into.

In addition to these test structures, we are currently collecting quadron statistics of structures with intermediate densities. This will help us obtain understanding on the influence of structure on the quadron characteristics.

We are also currently extending this type of study to three-dimensional structures, focusing on numerically generated foam structures. By tessellating into the 3D quadrons, we intend to analyse their statistics as a function of different generation protocols that give rise to different structures. Foams can be represented as network structures with nodes connected by Plateau borders (edges), as can be seen in Fig. 1. Foams are special in that they give tetrahedral structures (Frenkel et al. 2008 and 2009). These structures will be generated using the Surface Evolver software (Brakke 2008 and Neethling and Cilliers 2003).

Other than the availability of a software that produces such structures, we consider foam structures because they represent very sparse structures, consequently, they will give us insight into their dual – very dense structures.

Acknowledgements

References

[1] Ball, R.C. and Blumenfeld, R. [2002] Stress field in granular systems: loop forces and potential formulation. *Physical Review Letters*, **88**, 115505.

[2] Blumenfeld, R. and Edwards, S.F. [2003] Granular entropy: explicit calculations for planar assemblies. *Physical Review Letters*, **90**, 114303.

[3] Blumenfeld, R. and Edwards, S.F. [2006] *The European Physical Journal E*, **19**, 23-30.

[4] Blumenfeld, R. [2008] On entropic characterization of granular materials. In: Aste, T., Tordesillas A. and Matteo T.D. (Eds.) *Lecture Notes in Complex Systems Vol. 8: Granular and Complex Materials*. Singapore, World Scientific, 43-53.

[5] Brakke, K. [2008] Surface Evolver, version 2.30, www.susqu.edu/brakke/evolver/evolver.html.

[6] Brandon, N.P. and Brett, D.J. [2006] Engineering porous materials for fuel cell applications. *Philosophical Transaction of the Royal Society A*, **364**, 147-159.

[7] Dullien, F.A.L. [1992] *Porous Media: Fluid Transport and Pore Structure*, Academic Press.

[8] Edwards, S.F. and Oakeshott, R.B. [1989] Theory of Powders. Physica A, **157**, 1080-1090.

[9] Frenkel, G., Blumenfeld, R., Grof Z. and King, P.R. [2008] Structural characterization and statistical properties of two-dimensional granular systems. *Physical Review E*, **77**, 041304.

[10] Frenkel, G., Blumenfeld, R., King, P.R. and Blunt, M.J.[2009] Topological analysis of foams and tetrahedral structures. *Advanced Engineering Materials*, **11**, 169-176.

[11] Neethling, S.J. and Cilliers, J.J. [2003] Modelling flotation froths. *International Journal of Mineral Processing*, **72**, 267-287